International Journal of Creative and Open Research in Engineering and Management
ISSN: **3108-1754 (Online)**
Volume 02 Issue 06 June-2026 | Impact Factor: 3.5

Spatio-Temporal Dynamics of Summer Land Surface Temperature, Vegetation Cooling Effect, and Urban Heat Island Characteristics in Jammu Province, Western Himalaya (2000–2025)

Rakesh verma[1]
Meenu Sharma[2]

[1].Jammu and Forest Services, India
[2] Department of Geology, Cluster University of Jammu, Jammu 180001, India
∗Corresponding author. e-mail: *rakeshforests@gmail.com*

How to Cite this Article:

verma, R. & Sharma, M. (2026). Spatio Temporal Dynamics of Summer Land Surface Temperature, Vegetation Cooling Effect, and Urban Heat Island Characteristics in Jammu Province, Western Himalaya (2000–2025). International Journal of Creative and Open Research in Engineering and Management, <i>02</i>(6). https://doi.org/10.55041/ijcope.v2i6.321

License:

This article is published under the terms of the Creative Commons Attribution 4.0 International License (CC BY 4.0), which permits unrestricted use, distribution, and reproduction in any medium, provided the original author(s) and the source are credited.

© The Author(s). Published by International Journal of Creative and Open Research in Engineering and Management.

https://doi.org/ 10.55041/ijcope.v2i6.321

Abstract

Land surface temperature (LST) is a key indicator of environmental change and urban thermal stress, particularly in rapidly transforming mountain landscapes. This study investigates the spatio-temporal dynamics of summer LST, vegetation greenness, vegetation cooling effects, and urban heat island (UHI) characteristics across Jammu Province, Western Himalaya, from 2000 to 2025 using MODIS-derived LST (MOD11A2) and NDVI (MOD13Q1) products processed in Google Earth Engine (GEE; Wan, 2014; Didan, 2015; Gorelick et al., 2017). Annual summer (May–July) composites were generated, and long-term thermal trends were quantified using Sen's slope estimator, while NDVI–LST regressions quantified vegetation cooling effects and NDVI–LST coupling (Kendall, 1975; Sen, 1968). LST values were converted from scaled MOD11A2 digital numbers to degrees Celsius using a 0.02 scale factor and a Kelvin–Celsius offset, and NDVI was rescaled from MOD13Q1 using a 0.0001 scale factor (Wan, 2014; Didan, 2015; LP DAAC, 2021). Results show a gradual decline in mean summer LST from approximately 25.1 °C in 2000 to 23.7 °C in 2025 (−1.4 °C, ≈−0.056 °C yr^{-1}), while mean NDVI increased from 0.447 to 0.516 (≈15.4% increase in greenness). Histogram analysis indicates that most of Jammu Province experiences summer LST between 20 °C and 32 °C, with localized thermal hotspots (>30 °C) concentrated in low-elevation urban and industrial zones. Sen's slope analysis reveals that most pixels exhibit stable to cooling trends, with slopes predominantly between −0.10 and 0.00 °C yr^{-1}. A strong negative NDVI–LST relationship confirms the substantial cooling influence of vegetation, indicating that increased vegetation cover has mitigated regional thermal stress. The findings highlight the importance of afforestation, urban greening, and ecosystem-based adaptation in mitigating UHI intensity and enhancing climate resilience in the Western Himalayan region.

Keywords: land surface temperature; NDVI; urban heat island; vegetation cooling effect; Google Earth Engine; MODIS; Jammu Province; Western Himalaya, summer land surface temperature.

1. Introduction

Rapid urbanization, land-use change, and climate variability have altered surface thermal environments worldwide, leading to widespread emergence of the urban heat island (UHI) phenomenon, wherein urban areas exhibit higher temperatures than their rural surroundings due to increased impervious surfaces, anthropogenic heat emissions, and reduced vegetation cover (Oke, 1982; Voogt & Oke, 2003; Weng, 2009). Elevated LST amplifies heat stress, energy demand, air pollution, and heat-related morbidity and mortality, particularly during summer heat waves (Santamouris, 2014; Peng et al., 2012).

Mountain regions such as the Western Himalaya are especially sensitive to environmental change due to steep climatic gradients, ecological fragility, and rapid expansion of urban centers and infrastructure (Palazzi et al., 2013). Jammu Province, located at the southern foothills of the Western Himalaya, has experienced significant land-use transitions over the last two decades, including urban expansion, industrial growth, transport development, agricultural intensification, and forest management interventions. These changes can substantially modify the surface energy balance, yet the net effect on regional thermal regimes remains poorly quantified.

Vegetation plays a central role in regulating land surface temperatures through shading, evapotranspiration, and enhancement of soil moisture, thereby reducing sensible heat fluxes (Bonan, 2008; Bowler et al., 2010). Numerous studies have documented strong inverse relationships between vegetation indices such as the normalized difference vegetation index (NDVI) and LST in a variety of climatic settings, highlighting vegetation's cooling effect and its potential to mitigate UHI intensity (Mildrexler et al., 2011; Schwarz et al., 2012; Li et al., 2018). However, long-term assessments of NDVI–LST coupling, vegetation cooling effects, and UHI evolution remain scarce for Jammu Province despite its ecological and socio-economic importance.

The availability of continuous MODIS LST and vegetation index products, combined with cloud-based processing platforms such as Google Earth Engine (GEE), enables long-term, spatially explicit evaluation of surface temperature and vegetation dynamics at regional scale (Wan, 2014; Didan, 2015; Gorelick et al., 2017). Robust non-parametric trend techniques such as Sen's slope and Mann–Kendall tests allow quantification of monotonic thermal trends that are resistant to outliers and non-normality (Kendall, 1975; Sen, 1968; Yue et al., 2002).

The specific objectives of this study are to:

1. *Analyze temporal variations in summer LST (2000–2025) over Jammu Province using MODIS LST composites.*

2. *Assess vegetation dynamics using MODIS-derived NDVI.*

3. *Quantify vegetation cooling effects using NDVI–LST correlations and regressions.*

4. *Identify thermal hotspots and UHI characteristics.*

5. *Evaluate long-term thermal trends using Sen's slope analysis.*

6. *Discuss how summer temperature variation affects forest, urban, and rural environmental health within the area of interest (AOI).*

2. Study Area

Jammu Province occupies the southern part of the Union Territory of Jammu and Kashmir, India, extending from the Shivalik foothills in the south to the Pir Panjal range in the north. Elevations range from about 300 m in the plains to over 4,500 m above mean sea level in high-altitude terrain, encompassing subtropical, temperate, and cold temperate climatic regimes. The climate is characterized by hot summers, monsoon-influenced rainfall, and relatively moderate winters at lower elevations, with cooler conditions at higher altitudes.

Land cover is heterogeneous, comprising dense and open forests, scrublands, croplands, grasslands, river valleys, barren rocky slopes, and expanding urban and peri-urban settlements. Major urban centers such as Jammu City, Kathua, Samba, Udhampur, and Rajouri act as administrative and commercial hubs and represent potential UHI cores due to increasing built-up intensity and traffic. This complex interplay of topography, climate, and land use makes the province an ideal case for examining NDVI–LST interactions and UHI characteristics in a mountainous environment.

3. Materials and Methods

3.1 Data Sources

3.1.1 MODIS LST (MOD11A2)

The Terra MODIS Land Surface Temperature and Emissivity 8-day product (MOD11A2, Collection 6.1) provides average 8-day LST at 1 km spatial resolution on a 1,200 × 1,200 km sinusoidal grid (Wan, 2014; Wan et al., 2015). Each pixel value is a simple average of clear-sky daily LST estimates from MOD11A1 for the compositing period. MOD11A2 LST values are stored as scaled digital numbers (DN) in Kelvin and require a scale factor of 0.02 and a Kelvin–Celsius offset (273.15) to convert to degrees Celsius (Wan, 2014; LP DAAC, 2021).

3.1.2 MODIS NDVI (MOD13Q1)

The Terra MODIS Vegetation Indices product (MOD13Q1, Collection 6.1) provides 16-day NDVI and enhanced vegetation index (EVI) at 250 m spatial resolution (Didan, 2015). NDVI values are stored as scaled integers with a 0.0001 scale factor and are rescaled to obtain standard NDVI values in the range −1 to +1 (Didan, 2015; LP DAAC, 2021).

3.1.3 Digital Elevation Model

The Shuttle Radar Topography Mission (SRTM) 30 m digital elevation model (DEM; Farr et al., 2007) was used to interpret altitudinal gradients in LST and NDVI and to support visualization of topographic controls on thermal patterns.

3.1.4 Administrative Boundary

An administrative boundary shapefile for Jammu Province was used to clip all raster datasets to the provincial extent.

3.2 Pre-Processing and Summer Composites

All datasets were processed in Google Earth Engine (GEE), which enables scalable handling of multi-year satellite archives (Gorelick et al., 2017).

3.2.1 LST Conversion from MODIS DN to °C

For each MOD11A2 image, LST was converted from scaled DN to degrees Celsius using:

$$\mathrm{LST}\ (^\circ\mathrm{C}) = (\mathrm{DN}_{\mathrm{LST}} \times 0.02) - 273.15$$

where $\mathrm{DN}_{\mathrm{LST}}$ is the MOD11A2 LST digital number in Kelvin units and 0.02 is the scale factor specified in the product documentation (Wan, 2014; LP DAAC, 2021).

3.2.2 NDVI Rescaling from MODIS DN

For each MOD13Q1 image, NDVI was converted to dimensionless NDVI values as:

$$\mathrm{NDVI} = \mathrm{DN}_{\mathrm{NDVI}} \times 0.0001$$

where $\mathrm{DN}_{\mathrm{NDVI}}$ is the MOD13Q1 NDVI digital number and 0.0001 is the scale factor (Didan, 2015; LP DAAC, 2021).

3.2.3 Summer Seasonal Composites (May–July)

For each year y (2000–2025), all MOD11A2 and MOD13Q1 images corresponding to May, June, and July were filtered in GEE. A median composite was computed to represent mean summer conditions and to reduce the influence of residual clouds and outliers. Annual summer mean LST and NDVI were then calculated for the AOI as:

$$\bar{\mathrm{LST}}_y = \frac{1}{N_y} \sum_{i=1}^{N_y} \mathrm{LST}_{y,i}$$

$$\bar{\mathrm{NDVI}}_y = \frac{1}{M_y} \sum_{j=1}^{M_y} \mathrm{NDVI}_{y,j}$$

where N_y and M_y are the numbers of valid pixels for summer LST and NDVI in year y, respectively.

NDVI was aggregated to the 1 km LST grid using mean resampling to enable pixel-wise NDVI–LST comparison.

3.3 Trend Analysis Using Sen's Slope

Long-term thermal trends were quantified using Sen's slope estimator, a non-parametric method widely applied to hydro-climatic time series (Sen, 1968; Yue et al., 2002). For each pixel, pairwise slopes between all pairs of years i and j were computed as:

$$Q_{ij} = \frac{\mathrm{LST}_j - \mathrm{LST}_i}{j - i}, j > i$$

Sen's slope β_{Sen} is the median of all Q_{ij}:

$$\beta_{\mathrm{Sen}} = \mathrm{median}(Q_{ij})$$

Positive β_{Sen} values indicate warming trends, negative values indicate cooling trends, and values near zero indicate stable conditions. In this study, β_{Sen} values between −0.10 and 0.00 °C yr^{-1} were interpreted as stable to cooling trends at pixel level.

An AOI-scale average cooling rate was also approximated as:

$$\text{Cooling Rate} = \frac{\Delta \text{LST}}{\Delta t} = \frac{\text{LST}_{2025} - \text{LST}_{2000}}{2025 - 2000}$$

3.4 NDVI–LST Relationship and Vegetation Cooling Effect

The NDVI–LST relationship was quantified at both annual and pixel scales.

3.4.1 Pearson Correlation

Pearson's correlation coefficient r between NDVI and LST was computed as:

$$r = \frac{\sum_{k=1}^{n} (\text{NDVI}_k - \bar{\text{NDVI}})(\text{LST}_k - \bar{\text{LST}})}{\sqrt{\sum_{k=1}^{n} (\text{NDVI}_k - \bar{\text{NDVI}})^2} \sqrt{\sum_{k=1}^{n} (\text{LST}_k - \bar{\text{LST}})^2}}$$

where n is the number of pixels or annual observations. Negative values of r indicate that higher NDVI is associated with lower LST.

3.4.2 Linear Regression: Vegetation Cooling Effect

A simple linear regression model was applied:

$$\text{LST} = \alpha + \beta \cdot \text{NDVI} + \varepsilon$$

where α is the intercept and β is the slope (°C change per unit NDVI). A negative β indicates a cooling effect of vegetation, quantifying the decrease in LST per unit increase in NDVI (Li et al., 2018; Zhao et al., 2014).

3.5 Urban Hotspot and UHI Analysis

Surface UHI (SUHI) intensity was approximated as the difference between mean urban and rural LST (Chakraborty & Lee, 2019; Peng et al., 2012):

$$\text{SUHI}_{\text{int}} = \bar{\text{LST}}_{\text{urban}} - \bar{\text{LST}}_{\text{rural}}$$

where $\bar{\text{LST}}_{\text{urban}}$ and $\bar{\text{LST}}_{\text{rural}}$ are mean summer LST values of urban and rural pixels, respectively.

Thermal hotspots were defined as pixels with summer LST > 30 °C:

$$\text{Hotspot} = \{\text{pixels} \mid \text{LST} > 30\ ^{\circ}\text{C}\}$$

This threshold is consistent with approaches that define significant thermal anomalies relative to regional conditions (Imhoff et al., 2010; US EPA, 2014). The percentage of hotspot area was calculated as:

$$\%\text{Hotspot Area} = \frac{N_{\text{hotspot}}}{N_{\text{total}}} \times 100$$

where N_{hotspot} is the number of hotspot pixels and N_{total} is the total number of AOI pixels.

4. Results

4.1 Summer LST Trends (2000–2025)

The annual mean summer LST time series exhibits pronounced interannual variability superimposed on a modest cooling trend. The highest provincial mean summer LST occurred in 2002 (≈26.1 °C), while the lowest occurred in 2023 (≈21.8 °C). Over the study period, mean summer LST decreased from approximately 25.1 °C in 2000 to 23.7 °C in 2025, implying:

$$\Delta\text{LST} = 23.7 - 25.1 = -1.4\ °\text{C}$$

The corresponding AOI-scale cooling rate is:

$$\text{Cooling Rate} \approx \frac{-1.4}{25} = -0.056\ °\text{C yr}^{-1}$$

Representative summer mean LST values for selected years are shown in Table 1.

Table 1. Representative summer mean LST (°C) in Jammu Province.

Year	Mean LST (°C)
2000	24.8
2005	23.6
2010	24.5
2015	23.6
2020	24.3
2025	22.9

The fitted trend line confirms a gradual decline in summer LST, consistent with predominantly negative or near-zero Sen's slope values at pixel level.

4.2 NDVI Dynamics and Vegetation Trends

Summer NDVI increased steadily across Jammu Province during 2000–2025. Mean NDVI rose from 0.447 in 2000 to 0.516 in 2025:

$$\Delta\text{NDVI} = 0.516 - 0.447 = 0.069$$

The relative increase is:

$$\%\Delta \text{NDVI} = \frac{0.069}{0.447} \times 100 \approx 15.44\%$$

This indicates substantial greening over the 26-year period. Representative NDVI values for selected years are presented in Table 2.

Table 2. Representative summer mean NDVI in Jammu Province.

Year	Mean NDVI
2000	0.447
2005	0.452
2010	0.435
2015	0.466
2020	0.504
2025	0.516

Spatially, higher NDVI values correspond to forested uplands, riparian zones, and irrigated agricultural areas, while lower NDVI values are associated with urban cores, barren slopes, and sparsely vegetated terrain.

4.3 Vegetation Cooling Effect: NDVI–LST Relationship

Correlation and regression analyses reveal a strong negative relationship between NDVI and LST. Years with higher mean NDVI exhibit lower mean summer LST, and pixel-scale scatter plots show that high-NDVI areas systematically correspond to cooler LST.

The regression model:

$$\text{LST} = \alpha + \beta \cdot \text{NDVI} + \varepsilon$$

exhibits a negative slope β, confirming that increased vegetation greenness is associated with reduced summer LST. The magnitude of β quantifies the vegetation cooling effect in °C per unit NDVI, while a strong negative Pearson correlation coefficient r further supports the inverse NDVI–LST coupling (Li et al., 2018; Zhao et al., 2014). These relationships demonstrate that vegetation acts as a natural cooling mechanism, buffering surface thermal conditions in Jammu Province.

4.4 Temperature Distribution and Urban Hotspots

Histogram analysis indicates that most summer LST values fall between 20 °C and 32 °C. The dominant classes are 20–24 °C and 24–28 °C in vegetated and higher-elevation regions, while 28–32 °C values dominate in low-lying plains and more heavily urbanized landscapes. Pixels with LST > 30 °C constitute thermal hotspots.

These hotspots are concentrated in and around Jammu City, Kathua, Samba, Udhampur, Rajouri, and adjacent industrial and transport corridors, consistent with typical SUHI patterns (Imhoff et al., 2010; Peng et al., 2012). The proportion of hotspot area is relatively small compared to the full AOI, indicating that urban thermal anomalies are spatially localized rather than extensive.

4.5 Sen's Slope Spatial Thermal Trends

Sen's slope analysis shows that most pixels in Jammu Province exhibit negative to near-zero thermal trends. The majority of β_{Sen} values lie between −0.10 and 0.00 °C yr^{-1}, indicating stable to cooling summer LST conditions. Forest and agricultural landscapes predominantly show negative Sen's slope values, while limited patches with positive β_{Sen} (warming) occur in rapidly urbanizing or industrializing corridors, coinciding with observed hotspots.

These spatial patterns confirm that, overall, the province has experienced net cooling during summer despite localized warming in urban centers.

5. Discussion

5.1 Regional Cooling Versus Global Urban Warming

In contrast to many rapidly urbanizing regions where intensified warming and expanding UHIs are reported, Jammu Province exhibits an overall decline in summer LST alongside increased vegetation greenness. The net cooling of −1.4 °C over 26 years and the average cooling rate of −0.056 °C yr^{-1} suggest that ecosystem restoration, forest conservation, and agricultural greening have collectively offset the warming influence of urban expansion (Bonan, 2008; Imhoff et al., 2010; Li et al., 2018).

This finding highlights that regional-scale thermal trajectories reflect the combined effects of land-use change, vegetation dynamics, and topography, and that substantial vegetation enhancement can counteract local increases in impervious surfaces and anthropogenic heat.

5.2 Vegetation Cooling and Forest Health

The 15.4% increase in NDVI and the strong negative NDVI–LST relationship indicate that vegetation plays a central role in moderating thermal stress across the AOI. Increased tree cover and vegetated surfaces reduce LST through enhanced evapotranspiration and shading, consistent with numerous studies on the cooling effect of urban and peri-urban vegetation (Bowler et al., 2010; Zhao et al., 2014; Li et al., 2018).

For forested areas, lower summer LST (20–28 °C) supports physiological processes, promotes growth, and reduces heat-induced stress, while cooling trends and greening likely enhance forest resilience against extreme heat, drought, and wildfire risk (Hallett et al., 2022). However, localized hotspots near forest–urban interfaces may stress edge vegetation and increase vulnerability to pests and diseases (Hallett et al., 2022; Pretzsch et al., 2017).

Overall, forests in Jammu Province appear to benefit from both increased greenness and declining summer LST, suggesting a favorable trajectory for forest health at landscape scale.

5.3 UHI, Urban Hotspots, and Urban Environmental Health

Despite regional cooling, SUHI effects are evident in major urban centers, where LST exceeds 30 °C in localized hotspots. SUHI intensity, defined as the difference between mean urban and rural LST, is positive in cities such as Jammu and Kathua, reflecting warmer urban surfaces compared to rural surroundings (Chakraborty & Lee, 2019; Imhoff et al., 2010; Peng et al., 2012).

These urban hotspots have implications for:

- Increased thermal stress and risk of heat-related illnesses among urban populations (Santamouris, 2014).
- Higher energy demand for cooling and associated greenhouse gas emissions (Santamouris, 2014).
- Heightened heat and drought stress on urban trees compared to rural trees, potentially reducing urban tree health and ecosystem service delivery (Hallett et al., 2022; Urban et al., 2022).

However, the documented increase in NDVI and strong vegetation cooling effect indicate that urban and peri-urban greening can effectively reduce SUHI intensity and improve thermal comfort (Bowler et al., 2010; Zhao et al., 2014). Strategic urban tree planting, park creation, and green corridors are therefore critical adaptation measures for UHI mitigation in Jammu's cities.

5.4 Rural Environmental Health and Agricultural Resilience

Rural areas in Jammu Province, characterized by moderate summer LST and rising NDVI, exhibit favorable conditions for agriculture and rural vegetation. Moderate temperatures and enhanced vegetation cover reduce heat stress on crops and livestock, maintain soil moisture, and improve soil structure (Lobell & Gourdji, 2012). Cooling trends and increased greenness suggest that rural landscapes are becoming more resilient to thermal stress compared to many global regions experiencing intensifying heat extremes.

This improved thermal environment, combined with vegetation enhancement, provides an opportunity for sustainable agricultural intensification and integrated landscape management in the province.

5.5 Methodological Considerations and Limitations

MODIS products provide consistent, long-term coverage but are constrained by their relatively coarse spatial resolution. The 1 km resolution of MOD11A2 can mask fine-scale urban heterogeneity and small green spaces that significantly influence local micro-climates (Wan, 2014; Imhoff et al., 2010). MOD13Q1 NDVI may exhibit saturation in dense forests and is sensitive to soil background and atmospheric effects (Didan, 2015; Huete et al., 2002).

Cloud contamination and data gaps, although reduced by using median composites, may still affect certain years or locations. LST is not identical to near-surface air temperature, though numerous studies have demonstrated strong relationships between MODIS LST and air temperature across diverse environments (Mildrexler et al., 2011; Peng et al., 2012).

Future research could integrate higher-resolution sensors (e.g., Landsat, Sentinel-3), apply explicit significance testing (e.g., Mann–Kendall), and incorporate additional climatic drivers (precipitation, soil moisture) to refine trend attribution and improve understanding of the mechanisms underlying NDVI–LST dynamics.

- **Figure 1.** Summer mean LST trend (2000–2025) derived from MOD11A2 over Jammu Province.

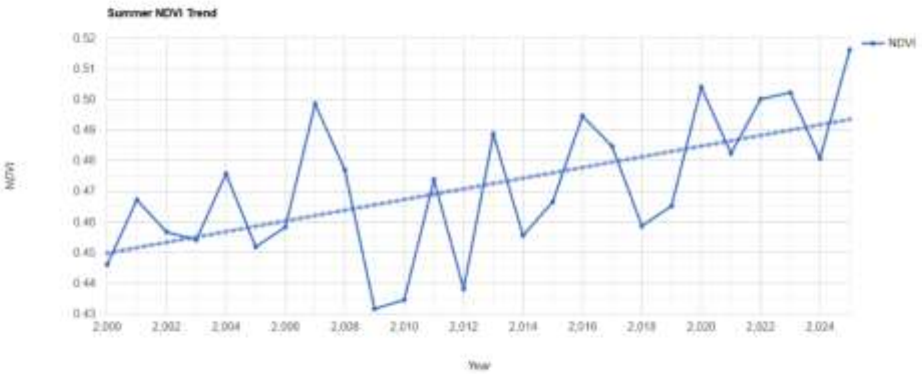

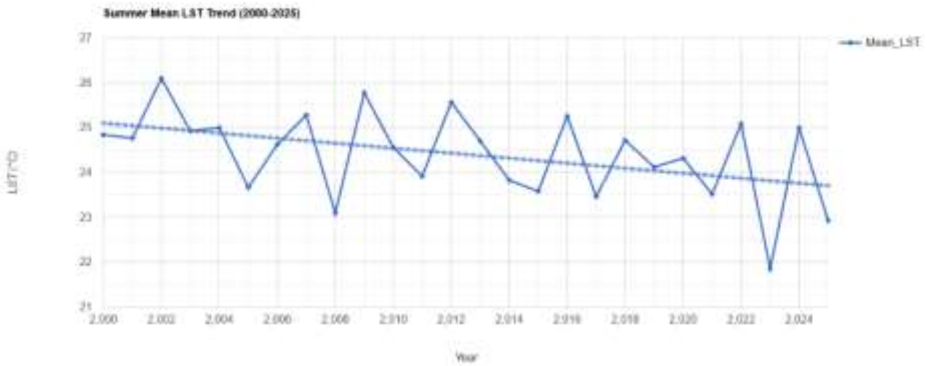

- **Figure 2.** Summer NDVI trend (2000–2025) derived from MOD13Q1 over Jammu Province.

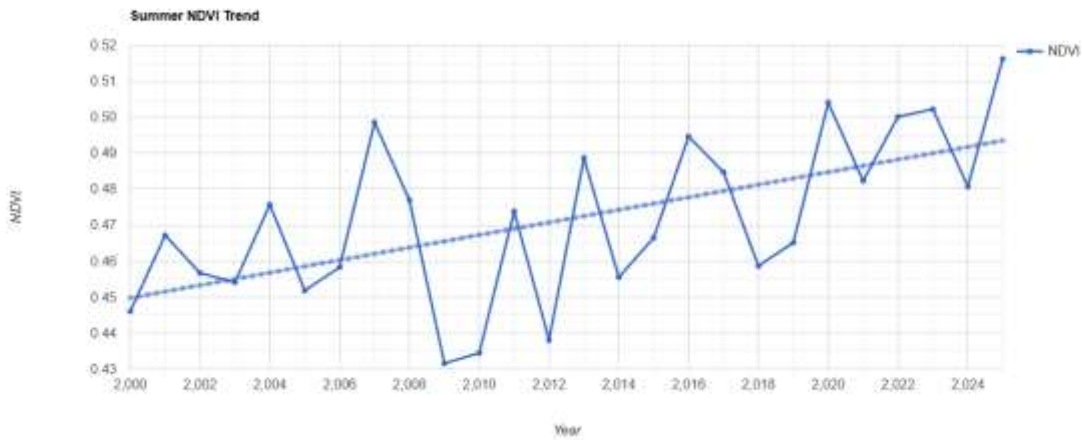

- **Figure 3.** NDVI–LST scatter plot and regression line illustrating vegetation cooling effect.

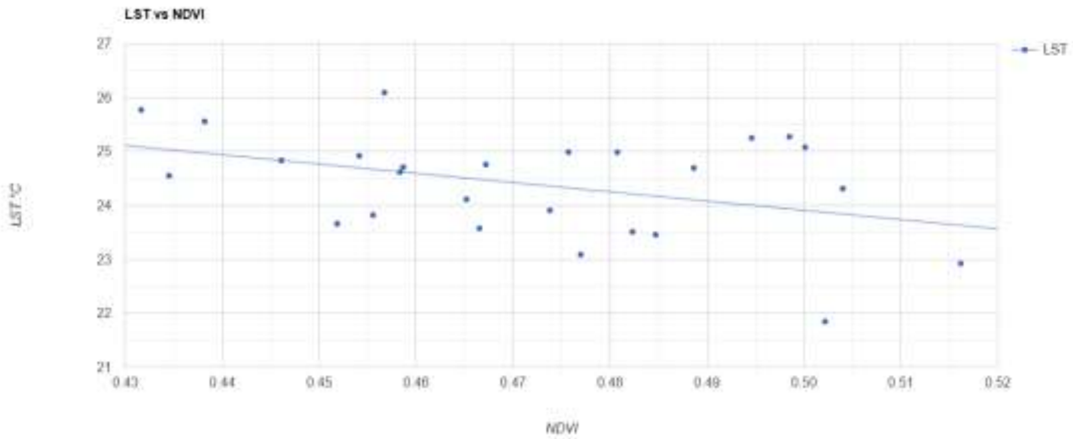

- **Figure 4.** Spatial distribution of summer LST with temperature classes (20–24 °C, 24–28 °C, 28–32 °C, >32 °C).

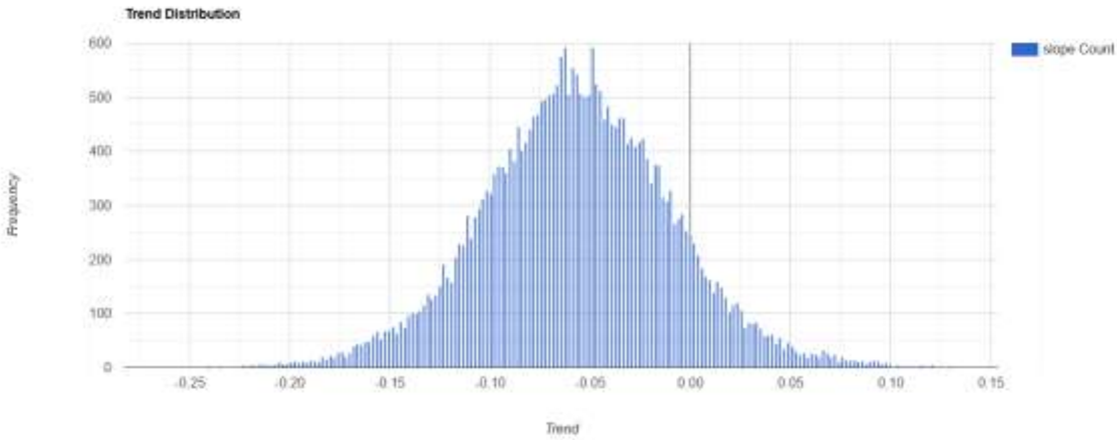

- **Figure 5.** Sen's Slope map of summer LST trends (°C yr⁻¹) showing spatial patterns of warming and cooling.

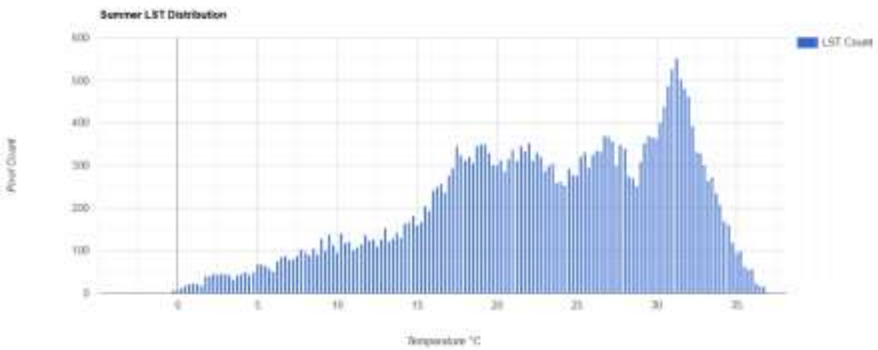

- **Figure 6.** Thermal hotspots (LST > 30 °C) and UHI zones in major urban centers and industrial corridors.

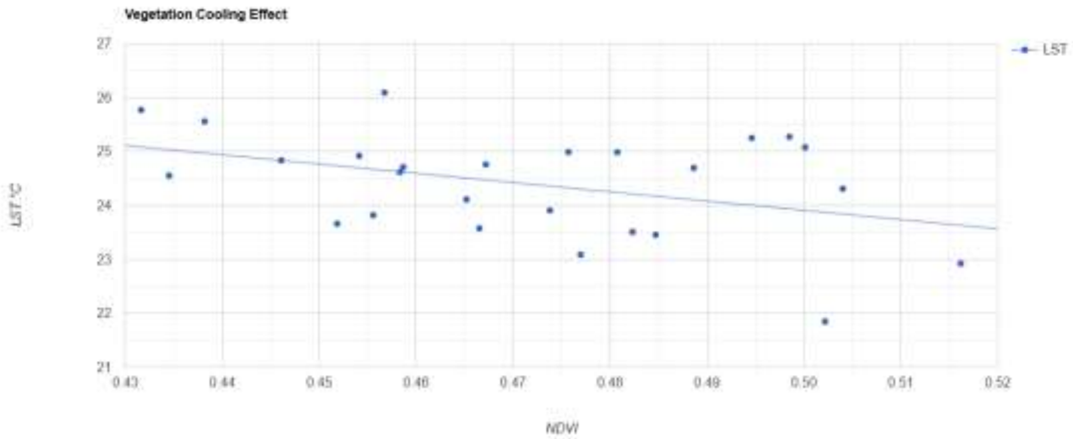

6. Conclusions

Using MODIS LST (MOD11A2) and NDVI (MOD13Q1) products processed in Google Earth Engine, this study provides a comprehensive assessment of summer LST dynamics, vegetation greenness, vegetation cooling effects, and UHI characteristics in Jammu Province, Western Himalaya, between 2000 and 2025 (Wan, 2014; Didan, 2015; Gorelick et al., 2017). The main conclusions are:

1. Summer LST cooling: Mean summer LST decreased from approximately 25.1 °C to 23.7 °C (−1.4 °C), corresponding to an average cooling rate of about −0.056 °C yr^{-1}.
2. Vegetation greening: Summer NDVI increased from 0.447 to 0.516 (≈15.4% increase), indicating substantial vegetation enhancement across the province.
3. Vegetation cooling effect: A strong negative NDVI–LST relationship and negative regression slope confirm that vegetation exerts a pronounced cooling influence on land surface temperatures.
4. Thermal distribution and hotspots: Most of the AOI falls within 20–32 °C summer LST classes, with hotspots (LST > 30 °C) localized in low-elevation urban and industrial landscapes, representing SUHI cores.
5. Sen's slope trends: Sen's slope analysis shows predominantly stable to cooling thermal trends (−0.10 to 0.00 °C yr^{-1}) across the AOI, with only limited warming patches in rapidly urbanizing corridors.
6. Implications for forest, urban, and rural health: Increased NDVI and cooling trends enhance forest and rural ecosystem resilience, while localized urban hotspots underscore the need for targeted urban greening and heat-health strategies.

These findings highlight the potential of vegetation-based climate adaptation—afforestation, ecosystem restoration, and urban greening—to mitigate UHI intensity and promote thermal resilience in the Western Himalayan region. The approach presented here can be replicated in other mountain regions to assess vegetation–temperature interactions and inform evidence-based adaptation policy.

References

Bonan, G. B. (2008). Forests and climate change: Forcings, feedbacks, and the climate benefits of forests. *Science, 320*(5882), 1444–1449.

Bowler, D. E., Buyung-Ali, L., Knight, T. M., & Pullin, A. S. (2010). Urban greening to cool towns and cities: A systematic review of the empirical evidence. *Landscape and Urban Planning, 97*(3), 147–155.

Chakraborty, T., & Lee, X. (2019). A simplified urban-extent algorithm to characterize surface urban heat islands on a global scale and examine vegetation control on their spatiotemporal variability. *International Journal of Applied Earth Observation and Geoinformation, 74*, 269–280.

Didan, K. (2015). *MOD13Q1 MODIS/Terra Vegetation Indices 16-Day L3 Global 250m SIN Grid V006* [Data set]. NASA EOSDIS Land Processes DAAC.

Farr, T. G., et al. (2007). The Shuttle Radar Topography Mission (SRTM). *Reviews of Geophysics, 45*(2), RG2004.

Gorelick, N., Hancher, M., Dixon, M., Ilyushchenko, S., Thau, D., & Moore, R. (2017). Google Earth Engine: Planetary-scale geospatial analysis for everyone. *Remote Sensing of Environment, 202*, 18–27.

Hallett, R. A., et al. (2022). Climate change and urban forests. In *Climate change and forests of the future* (pp. XX–XX). USDA Forest Service, Northern Research Station.

Huete, A., Didan, K., Miura, T., Rodriguez, E. P., Gao, X., & Ferreira, L. G. (2002). Overview of the radiometric and biophysical performance of the MODIS vegetation indices. *Remote Sensing of Environment, 83*(1–2), 195–213.

Imhoff, M. L., Zhang, P., Wolfe, R. E., & Bounoua, L. (2010). Remote sensing of the urban heat island effect across biomes in the continental USA. *Remote Sensing of Environment, 114*(3), 504–513.

Kendall, M. G. (1975). *Rank correlation methods* (4th ed.). Charles Griffin.

Li, X., Zhou, Y., Asrar, G. R., Imhoff, M., & Li, X. (2018). The surface urban heat island response to urban expansion: A panel analysis for the conterminous United States. *Science of the Total Environment, 605–606*, 426–435.

Lobell, D. B., & Gourdji, S. M. (2012). The influence of climate change on global crop productivity. *Plant Physiology, 160*(4), 1686–1697.

LP DAAC. (2021). *MOD11A2, MOD13Q1 user guides and product documentation.* NASA EOSDIS Land Processes DAAC.

Mildrexler, D. J., Zhao, M., & Running, S. W. (2011). A global comparison between station air temperatures and MODIS land surface temperatures reveals the cooling role of forests. *Journal of Geophysical Research: Biogeosciences, 116*(G3), G03025.

Oke, T. R. (1982). The energetic basis of the urban heat island. *Quarterly Journal of the Royal Meteorological Society, 108*(455), 1–24.

Palazzi, E., von Hardenberg, J., & Provenzale, A. (2013). Precipitation in the Hindu-Kush Karakoram Himalaya: Observations and future scenarios. *Journal of Geophysical Research: Atmospheres, 118*(1), 85–100.

Peng, S., et al. (2012). Surface urban heat island across 419 global big cities. *Environmental Science & Technology, 46*(2), 696–703.

Pretzsch, H., et al. (2017). Climate change accelerates growth of urban trees in metropolises worldwide. *Scientific Reports, 7*, 15403.

Santamouris, M. (2014). On the energy impact of urban heat island and global warming on buildings. *Energy and Buildings, 82*, 100–113.

Schwarz, N., Lautenbach, S., & Seppelt, R. (2012). Exploring indicators for quantifying surface urban heat islands of European cities with MODIS land surface temperatures. *Remote Sensing of Environment, 115*(12), 3175–3186.

Sen, P. K. (1968). Estimates of the regression coefficient based on Kendall's tau. *Journal of the American Statistical Association, 63*(324), 1379–1389.

Urban, J., Ingwers, M. W., McPherson, E. G., & Simpson, J. R. (2022). Urban trees and climate change: Stressors, responses, and management. *Urban Forestry & Urban Greening, 68*, 127511.

US Environmental Protection Agency (US EPA). (2014). *How researchers measure urban heat islands.* US EPA Heat Island Reduction Program.

Voogt, J. A., & Oke, T. R. (2003). Thermal remote sensing of urban climates. *Remote Sensing of Environment, 86*(3), 370–384.

Wan, Z. (2014). *New refinements and validation of the MODIS land-surface temperature/emissivity products. Remote Sensing of Environment, 140*, 36–45.

Wan, Z., Hook, S., & Hulley, G. (2015). *MOD11A2 MODIS/Terra Land Surface Temperature/Emissivity 8-Day L3 Global 1km SIN Grid V006* [Data set]. NASA EOSDIS Land Processes DAAC.

Weng, Q. (2009). Thermal infrared remote sensing for urban climate and environmental studies: Methods, applications, and trends. *ISPRS Journal of Photogrammetry and Remote Sensing, 64*(4), 335–344.

Yue, S., Pilon, P., & Cavadias, G. (2002). Power of the Mann–Kendall and Spearman's rho tests for detecting monotonic trends in hydrological series. *Journal of Hydrology, 259*(1–4), 254–271.